PHYSICAL REVIEW C **91**, 032501(R) (2015)

High-precision half-life measurement for the isospin $T = 1/2$ mirror β^+ decay of ^{21}Na

J. Grinyer,[1,*] G. F. Grinyer,[1] M. Babo,[1] H. Bouzomita,[1] P. Chauveau,[1] P. Delahaye,[1] M. Dubois,[1] R. Frigot,[1] P. Jardin,[1] C. Leboucher,[1] L. Maunoury,[1] C. Seiffert,[2] J. C. Thomas,[1] and E. Traykov[1]

[1]*Grand Accélérateur National d'Ions Lourds (GANIL), CEA/DSM-CNRS/IN2P3, Bvd Henri Becquerel, 14076 Caen, France*

[2]*ISOLDE, CERN, 1211 Geneva 23, Switzerland*

(Received 30 October 2014; revised manuscript received 4 February 2015; published 24 March 2015)

The half-life of the isospin $T = 1/2$ mirror β^+ decay of ^{21}Na was measured at the GANIL-SPIRAL radioactive ion beam facility to be $T_{1/2} = 22.422\ (10)$ s, a result that is more than a factor of 5 times more precise than the previous world average, with a resulting ft value that is now two times more precise. The precision of this new result implies that the half-life is no longer the dominant source of uncertainty in the $\mathcal{F}t$ value used in the calculation of $V_{\rm ud}$ from mirror decays to test the conserved vector current hypothesis of the standard model. The value of $V_{\rm ud}$ deduced from mirror decays using the new half-life result is now in better agreement with the $V_{\rm ud}$ derived from $T = 1$ superallowed 0^+ to 0^+ transitions.

DOI: 10.1103/PhysRevC.91.032501 PACS number(s): 21.10.Tg, 23.40.−s, 27.30.+t

Introduction. The unitarity test of the Cabibbo-Kobayashi-Maskawa (CKM) quark mixing matrix is crucial for constraining possible extensions to the standard-model description of electroweak interactions. In particular, the up-down element of the matrix, $V_{\rm ud}$, which plays by far the dominant role, is presently obtained from measurements of superallowed 0^+ to 0^+ nuclear β decays [1]. Given the present uncertainty in the neutron lifetime [2,3], the second most precise value of $V_{\rm ud}$ is obtained from isospin $T = 1/2$ mirror β-decay transitions (mixed Fermi and Gamow-Teller) and thus provides a complementary method of obtaining $V_{\rm ud}$ [4]. The $\mathcal{F}t$ values for mirror transitions of ^{19}Ne, ^{21}Na, ^{29}P, ^{35}Ar, and ^{37}K are included in the average of $V_{\rm ud}$, since for these cases, both the experimental ft values and the correlation parameters are known with sufficient precision [4]. For $T = 1/2$ mirror decays, $\mathcal{F}t^{\rm mirror}$ and $V_{\rm ud}$ are related by [5]

$$\mathcal{F}t^{\rm mirror} = \frac{K}{G_F^2 V_{\rm ud}^2} \frac{1}{C_V^2 \left|M_F^0\right|^2 \left(1+\Delta_R^V\right)[1+(f_A/f_V)\rho^2]}, \tag{1}$$

where $K/(\hbar c)^6 = 2\pi^3 \ln 2 \hbar/(m_e c^2)^5 = 8120.271(12) \times 10^{-10}$ GeV^{-4}s, $G_F/(\hbar c)^3 = 1.1663787(6) \times 10^{-5}$ GeV^{-2} is the Fermi constant, $C_V = 1$ is the vector coupling constant, $|M_F^0|^2$ is the Fermi matrix element and takes the value of 1 for $T = 1/2$ transitions, Δ_R^V is a transition-independent radiative correction, f_A and f_V are statistical rate functions for axial-vector and vector currents, respectively, and ρ is the Gamow-Teller to Fermi mixing ratio. The value of ρ must be deduced experimentally from measurements of angular or asymmetry correlation parameters.

The primary quantity required to calculate $\mathcal{F}t^{\rm mirror}$ is the experimental ft value that is derived from three experimental quantities: the decay Q value, the branching ratio, and the half-life. The experimental ft value then has to be modified by several theoretical corrections for Coulomb and radiative effects that can be written as [5]

$$\mathcal{F}t^{\rm mirror} = ft(1+\delta_R')\left(1+\delta_{NS}^V-\delta_C^V\right), \tag{2}$$

where f is the statistical rate function, t is the partial half-life, δ_R' and δ_{NS}^V are nucleus-dependent radiative corrections, and δ_C^V is the isospin-symmetry breaking correction.

Unlike the set of the 14 most precisely determined $\mathcal{F}t$ values for $T = 1$ superallowed β emitters [1], the uncertainties in the $\mathcal{F}t^{\rm mirror}$ values are presently dominated by experimental sources [4] thereby prompting a need for new precise measurements for the ft values of $T = 1/2$ mirror β decays. This is particularly important for the five nuclei, ^{19}Ne, ^{21}Na, ^{29}P, ^{35}Ar, and ^{37}K, that are presently included in the determination of $V_{\rm ud}$ for mirror transitions. Of these five mirror nuclei, ^{19}Ne, ^{21}Na, and ^{35}Ar play a dominant role since the other transitions are not known with comparable precision. Several recent measurements of ^{19}Ne [6–8] have improved the half-life precision to 0.01% making it the most precisely known half-life for any $T = 1/2$ mirror decay. A recent half-life measurement of ^{37}K [9] has increased the precision of its $\mathcal{F}t^{\rm mirror}$ value four-fold; however, the poorly known value of ρ for this nucleus still limits its contribution in the calculation of $V_{\rm ud}$.

There has been renewed interest in the study of the β decay of ^{21}Na: both branching ratios and β-ν correlation parameters have been measured recently [10–12]; however, its experimental ft value has the lowest precision of the three mirror nuclei that dominate the determination of $V_{\rm ud}$. In particular, the $\mathcal{F}t^{\rm mirror}$ value for ^{21}Na is largely limited by the uncertainty in its half-life. There are three previous measurements [13–15] that yield an average half-life of 22.487 (54) s after applying a scaling factor to take into account the relatively large reduced χ^2 value of 3.6. The most recent value of 22.47 (3) s was obtained 40 years ago [15].

In this work, a high-precision half-life measurement of ^{21}Na was performed and a precise value of $\mathcal{F}t^{\rm mirror}$ was extracted, which causes a shift in the value of $V_{\rm ud}$ derived from mirror

*joanna.grinyer@ganil.fr

transitions and leads to an even better agreement with the value of V_{ud} derived from superallowed 0^+ to 0^+ decays. Our measurement of the ^{21}Na half-life, which is more than five times more precise, and the resulting precision of $\mathcal{F}t^{\text{mirror}}$ now paves the way for improving V_{ud} via correlation parameter measurements to deduce the Gamow-Teller to Fermi mixing ratio ρ.

Experiment. The experiment was performed at the SPIRAL (Système de Production d'Ions Radioactifs Accélérés en Ligne) rare-isotope beam facility at GANIL (Grand Accélérateur National d'Ions Lourds) in Caen, France. Radioactive ion beams were produced from the fragmentation of a 95 MeV/u primary $^{36}Ar^{18+}$ beam on a graphite target and were ionized in a VADIS-type (Versatile Arc Discharge Ion Source [16]) FEBIAD (Forced Electron Beam Ion Arc Discharge) ion source operating in its first online production run. Ions were extracted from the source at 10 kV and were separated based on their charge-to-mass ratio with a resolution of $m/\Delta m \approx 300$. Radioactive beams of ^{21}Na were delivered as $^{21}Na^{1+}$ at $A/q = 21$ with an average intensity of 4×10^7 ions/s to the SPIRAL low-energy identification and tape transport station [17]. Ions were implanted into an aluminized-Mylar tape in the collection chamber. A high-purity germanium (HPGe) detector, located at 0° with respect to the beam axis, was used for identification and to quantify and monitor the beam purity and intensity. Based on γ-ray spectra, there was no evidence of $A = 21$ isobars such as ^{21}O, ^{21}F, and ^{21}Mg. The only observed isobaric contaminant was the long-lived $^{42}K^{2+}$ ($T_{1/2} = 12.360$ h) delivered at 10^3 ions/s produced from the fragmentation of the ^{36}Ar primary beam on the Ta target window and not from the direct fragmentation on the graphite target.

After an implantation period in the collection chamber, the sample was transported to the decay chamber for the half-life measurement. Following the decay of implanted ^{21}Na nuclei, emitted positrons were detected using a 3 mm thick, $40 \times 40\,\text{mm}^2$ BC-404 fast plastic scintillator coupled to two photomultiplier tubes (PMTs) (Hamamatsu model R2248) biased at -300 V. The individual photomultiplier signals were discriminated and combined in a logical AND to reduce noise effects and the signals were sent to a multichannel scaler module. These scaler data were time-stamped using a 10 kHz precision clock. The scaler module is free running and is operated independently of the trigger used for the data acquisition. This module has been tested to function without losing events with input frequencies of up to 100 MHz, although in practice the count rate in experiments is limited to significantly less ($\approx$ 10 kHz). With this method, the raw data are directly used for analysis since no dead time or pile up corrections are required. This method was used recently at GANIL to deduce the half-life of ^{19}Ne to high precision (0.03%) [6].

Beam intensities were controlled using a series of attenuators in the beam line located 10 m upstream from the experimental station. The reduction factors were chosen so that the initial count rate in the scintillator did not exceed $\approx$ 10 kHz. A full description of the SPIRAL identification station, associated electronics, and further details about the SPIRAL low-energy facility can be found in Ref. [17].

Data were collected in cycles. A typical cycle consisted of a background collection time of 1 s, followed by a beam-on period between 2 and 14 s to implant ions on the tape, 3 s of tape movement were then required to move the sample from the implantation site to the measurement site in front of the scintillator, a 450 s decay counting period (approximately 20 half-lives of ^{21}Na), and 5 s of tape movement to remove long-lived contaminant activity away from the scintillator and into a shielded tape storage box before the start of the next cycle. The beam-on time was varied between 2 and 14 s in order to test for any possible sources of rate-dependent effects. The total data set consisted of 44 cycles collected over six experimental runs.

Half-life determination. Half-life results for ^{21}Na were obtained by performing fits to the decay activity curves using a modified Levenberg-Marquardt χ^2 minimization method described in previous publications [18,19]. Of the 44 cycles that were collected during the experiment, one cycle was rejected because the run was stopped early and the decay curve was incomplete (less than five half-lives of ^{21}Na). A total of 43 cycles from six runs were included in the analysis.

The half-life of ^{21}Na was deduced from the sum of the 43 independent decay curves obtained from the time-stamped scaler data. As described above, dead time losses are negligible at standard scaler operating conditions and thus no dead time corrections were applied to the raw data. The summed decay curve was fit (hereafter referred to as the "global fit" method) using a single exponential decay with a constant background for a total of three free parameters (assuming the ^{42}K activity is constant, see discussion below). The decay period of 450 s was chosen to be sufficiently long so that the constant background level could be well constrained in the fitting procedure. The start of the fit was chosen to be 1 s (1 channel) after the tape-drive motor was stopped (1 s from the start of the decay period) to ensure that the tape was fully stopped in front of the scintillator. The half-life of ^{21}Na was determined via the global fit method to be $T_{1/2} = 22.4218\ (92)$ s with a reduced χ^2/ν of 1.04, representing a statistical precision of 0.04%. The decay curve and the resulting best fit are shown in Fig. 1. The fit residuals (mean of -0.0002 and standard deviation of 1.02) are displayed in the lower panel of Fig. 1.

Systematic uncertainties. Several tests were performed to search for potential systematic effects that may bias the high-precision half-life result. As a first step, the fit to the summed decay curve (Fig. 1) was repeated by removing a number of leading channels (the high-rate data) from the analysis in a step-wise manner. The summed decay curve was fit in steps of 3 channels, and up to a total of 45 channels were removed (2 half-lives of ^{21}Na). The resulting half-life as a function of the number of leading channels removed is plotted in Fig. 2. Since these data are not independent but highly correlated due to the fact that leading channels are removed and the same data are re-fit, the data points are not expected to be scattered around a mean value. Nevertheless, this analysis is sensitive to rate-dependent sources of systematic uncertainty such as PMT gain shifts and detector after-pulsing [7], and to the presence of isobaric contaminants. Since the half-life of ^{21}Na remains constant as the high-rate data are removed, there is no

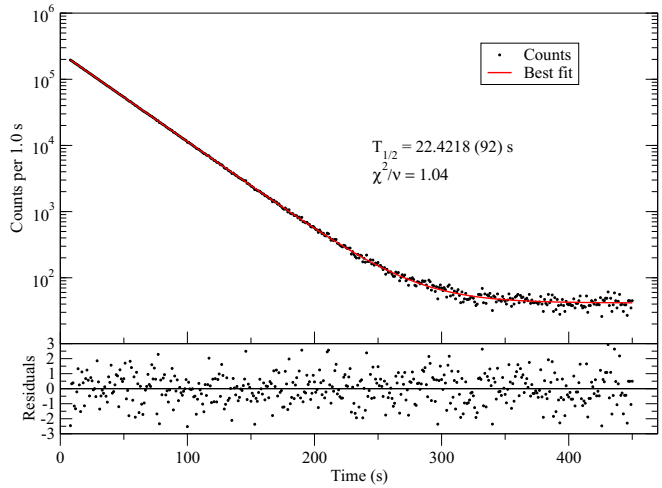

FIG. 1. (Color online) Decay curve of ^{21}Na and resulting global fit from the sum of all cycles and runs. The intensity of the fitted background is 41.6 (0.5) counts/s, representing a 0.97 (1) count/s background rate in the scintillator. The fit residuals $(y_i - y_{\rm fit})/\sigma_i$ are displayed in the lower panel (mean of −0.0002 with a standard deviation of 1.02).

evidence from this analysis that any rate-dependent sources of systematic uncertainty are present in the measurement.

The half-life and reduced χ^2 were also determined individually for each of the 43 cycles. Every cycle had a reduced χ^2 below 1.2, suggesting that no particular cycle or data subset was subject to any obvious sources of systematic uncertainty. The cycle-by-cycle half-life results are shown in Fig. 3 where the weighted average from the 43 cycles is 22.4210 (92) s with a reduced χ^2/ν of 1.19 for 42 degrees of freedom. A run-by-run analysis was also performed by summing all cycles belonging to a particular experimental run. The weighted average from the fit to each of the six runs is 22.4214 (91) s

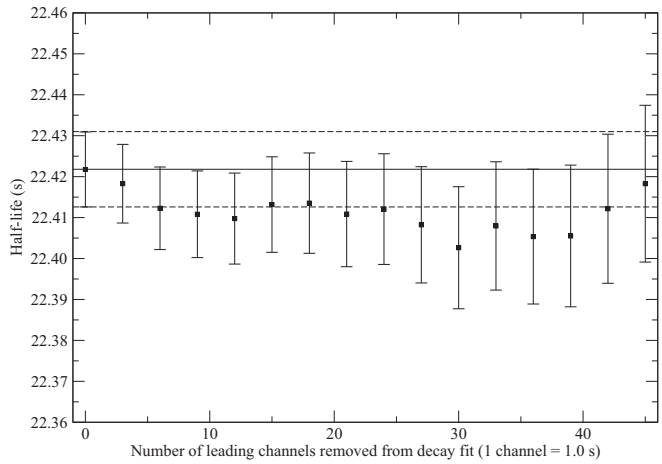

FIG. 2. Effect of removing an increasing number of leading channels on the ^{21}Na half-life (1 channel = 1.0 s) from the summed decay curve, with the half-life and uncertainty [22.4218 (92) s from Fig. 1] overlaid to guide the eye.

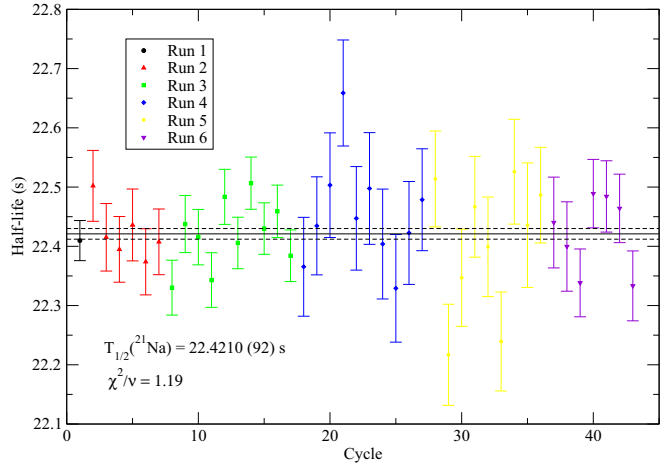

FIG. 3. (Color online) Half-life of ^{21}Na when data are analyzed on a cycle-by-cycle basis.

with a reduced χ^2 value of 0.35 for 5 degrees of freedom. The half-lives deduced on a run-by-run basis are shown in Fig. 4.

An additional test was performed to determine whether the beam-on time and hence the initial count rate in the scintillator could yield any bias in the deduced half-life. During the experiment, a total of four different beam-on settings were used: 2 s (2 runs), 4 s (2 runs), 7 s (1 run), and 14 s (1 run). These corresponded to a broad range of initial scintillator counting rates of 2.5, 5, 8, and 15 kHz, respectively. Runs were grouped according to beam-on time and the resulting weighted-average half-life of 22.4215 (91) s and reduced χ^2/ν of 0.06 (for 3 degrees of freedom) are shown in Fig. 5. Since there is no significant variation in the deduced half-life with beam-on time and hence initial scintillator count rate, any possible sources of rate-dependent systematic effects can be considered negligible compared to the statistical precision of the measurement. A summary of the results from the above search for systematic effects are presented in Table I. The results of the cycle-by-cycle, the run-by-run, and the counting

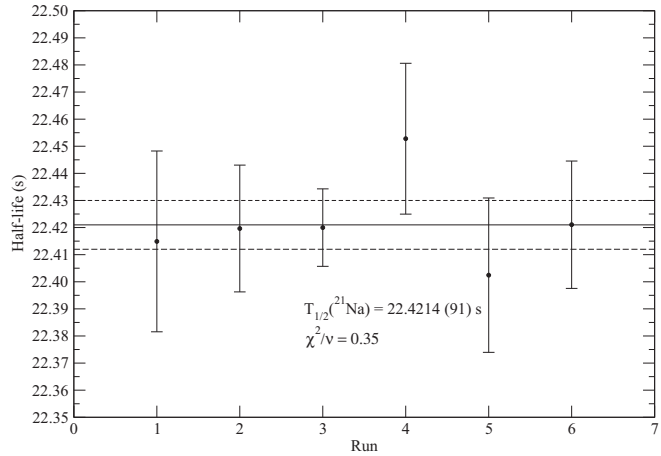

FIG. 4. Half-life of ^{21}Na when data are analyzed on a run-by-run basis.

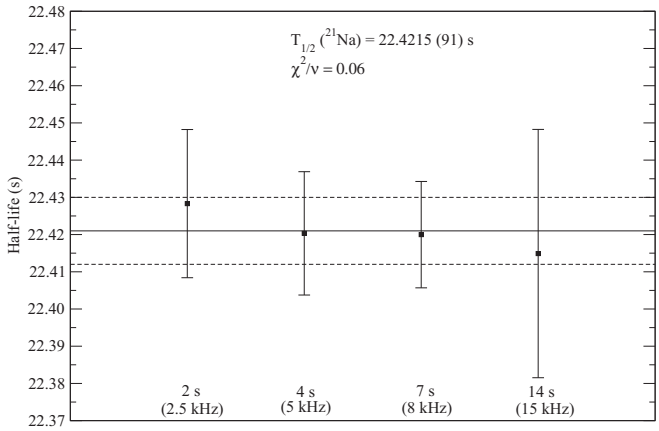

FIG. 5. Half-life of ^{21}Na as a function of beam-on time. Four beam-on settings were used: 2 s (representing a 2.5 kHz initial count rate in the scintillator), 4 s (5 kHz), 7 s (8 kHz), and 14 s (15 kHz). No systematic effect can be deduced from data sorted according to the beam-on time and thereby the counting rate.

rate variation analysis are all consistent with the global fit result.

The above analysis rules out the presence of potential sources of significant systematic uncertainties such as rate-dependent effects (for example PMT gain shifts and after-pulsing) and the presence of short-lived isobaric contaminants. As mentioned previously, the only known contaminant that was identified based on γ-ray spectra collected at the implantation site is ^{42}K, delivered as a 2+ ion at $A = 21$. In the above analysis, decay curves were fit using a single exponential decay for ^{21}Na, and a single constant background parameter that incorporates both the counter background and the ^{42}K ($T_{1/2} = 12.360$ h) long-lived component that was assumed to be constant on the 450 s time scale of the ^{21}Na measurement. The background rate of $\approx$1 count/s in the scintillator was deduced from dedicated background runs performed before, during, and after the present experiment. The background of 0.97(1) counts/s obtained from the free fit parameter of the global fit (Fig. 1) is thus consistent with the expected value. With a $^{42}K^{2+}$ beam intensity of 10^3 ions/s, only 0.05 counts/s (of the total 0.97 counts/s) are expected to come from $^{42}K^{2+}$. A Monte Carlo simulation was performed to test the assumption that the activity of ^{42}K can be treated as a constant background parameter. Decay curves of ^{21}Na were simulated with the total background rate of 0.97 counts/s including the rate of 0.05 counts/s expected from ^{42}K decay, and were fit using the same single exponential decay plus a single constant background

TABLE I. Summary of half-life results from the global fit and from different systematic effect tests.

Method	Half-life (s)
Global fit	22.4218 (92)
Cycle-by-cycle	22.4210 (92)
Run-by-run	22.4214 (91)
By rate	22.4215 (91)

TABLE II. Error budget for the ^{21}Na half-life measurement.

Source	Uncertainty (s)
Statistical	0.0092
Cycle-by-cycle χ^2/ν	0.0040
Background (^{42}K)	0.000016
Total	0.010

function as employed for the experimental data. The simulation indicated that the contribution of ^{42}K decay to the background changes the half-life by 0.000016 s when treated as a constant, which is $\approx$600 times less than the statistical precision. The assumption that the 0.05 counts/s of ^{42}K in the background can be approximated by a constant count rate over the 450 s time scale of the measurement is thus fully justified.

Since all analysis undertaken to search for possible rate-dependent sources of systematic effects yielded χ^2/ν values of less than 1 with the exception of the half-life derived from the global fit and those derived on a cycle-by-cycle basis, an overall systematic uncertainty can be estimated to account for all possible sources using the method of the Particle Data Group [20] in which the statistical uncertainty of $\pm$0.0092 s (global fit method) is increased by the square root of the largest χ^2/ν of 1.19 obtained from the cycle-by-cycle analysis. This method yields a total uncertainty of $\pm$0.010 s that is presently dominated by statistical uncertainties. A summary of all uncertainties is presented in Table II. The final result, precise to 0.04%, can be written as

$$T_{1/2} = 22.422(9)_{\text{stat}}(4)_{\text{syst}}\ \text{s}, \tag{3}$$

where the first uncertainty is statistical and the second is systematic. This result is in agreement with, but is more than five times more precise than the previous world average of 22.487 (54) s [5]. Using the averaging procedure adopted in Ref. [5], the new world average of ^{21}Na half-life is $T_{1/2} =$ 22.428 (14) s. A summary of all ^{21}Na half-life measurements performed to date is shown in Fig. 6.

$\mathcal{F}t^{\text{mirror}}$ value. With the new high-precision ^{21}Na half-life result, the $\mathcal{F}t^{\text{mirror}}$ value for ^{21}Na can now be calculated using Eq. (2), and the values of $\delta_R^{'}$, δ_{NS}^{V}, and δ_C^{V} from Ref. [5]. The result

$$\mathcal{F}t^{\text{mirror}} = 4073.3(62)\ \text{s}, \tag{4}$$

is two times more precise than the previous value from Ref. [4], and ^{21}Na now represents the second (after ^{19}Ne) most precisely determined $\mathcal{F}t^{\text{mirror}}$ value for any of the $T = 1/2$ mirror cases at 0.15% precision.

The improvement in the half-life precision resulting from the present work implies that the leading source of uncertainty in $\mathcal{F}t^{\text{mirror}}$ is now no longer the half-life, but the Q_{EC} value. The present status of the uncertainties on the quantities that contribute to the error budget of the $\mathcal{F}t^{\text{mirror}}$ values is shown in Fig. 7. The contributions to the error budget from ^{19}Ne, ^{35}Ar, and ^{37}K, the other most precisely known $T = 1/2$ mirror nuclei, are also shown for comparison.

In order to evaluate the impact of the new ^{21}Na half-life on the determination of V_{ud}, the corrected $\mathcal{F}t^{\text{mirror}}$, denoted

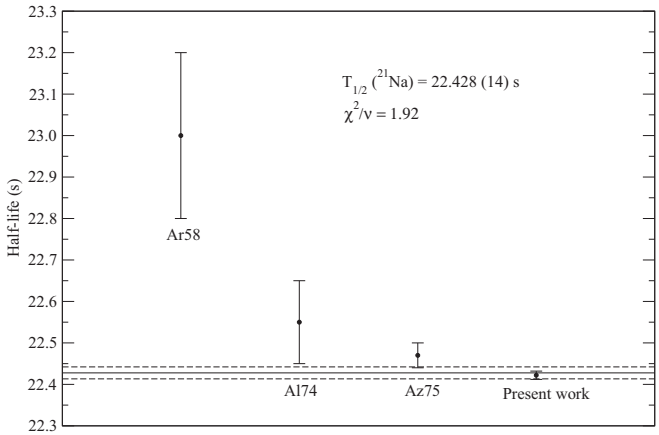

FIG. 6. Summary of all ^{21}Na half-life measurements. References to previous measurements are Ar58 [13], Al74 [14], and Az75 [15]. The weighted average of all results is 22.428 (14) s with a χ^2/ν of 1.92 for 2 degrees of freedom, following the averaging procedure described in Ref. [5].

$\mathcal{F}t_0$, must be determined. This corrected value removes the Gamow-Teller to Fermi mixing components to obtain the pure vector contribution and therefore is expected to be constant for all transitions. $\mathcal{F}t_0$ is defined by [5]

$$\mathcal{F}t_0 = \mathcal{F}t^{\text{mirror}}[1 + (f_A/f_V)\rho^2]. \quad (5)$$

The value of $\mathcal{F}t^{\text{mirror}}$ is taken from the present work [Eq. (4)], and the f_A/f_V ratio and ρ values are adopted from Refs. [4,5]. The resulting value of $\mathcal{F}t_0$ for ^{21}Na is determined to be

$$\mathcal{F}t_0 = 6184(46)\ \text{s}. \quad (6)$$

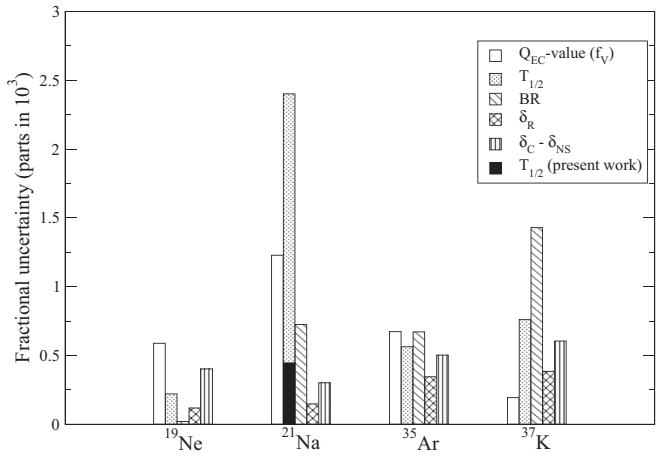

FIG. 7. Fractional uncertainties in $\mathcal{F}t^{\text{mirror}}$ of the experimental and theoretical quantities needed to calculate the $\mathcal{F}t^{\text{mirror}}$ value. The improvement in $T_{1/2}$ precision of ^{21}Na from the present work means the $T_{1/2}$ uncertainty no longer dominates the uncertainty in $\mathcal{F}t^{\text{mirror}}$. Three well-known mirror transitions, ^{19}Ne, ^{35}Ar, and ^{37}K, are shown for comparison. The values in the plot are adopted from Ref. [5], except the $T_{1/2}$ of ^{19}Ne and ^{37}K for which the most recent results [6–9] are included to calculate new world averages of 17.2579 (38) s and 1.23633 (94) s, respectively, following the method from Ref. [5].

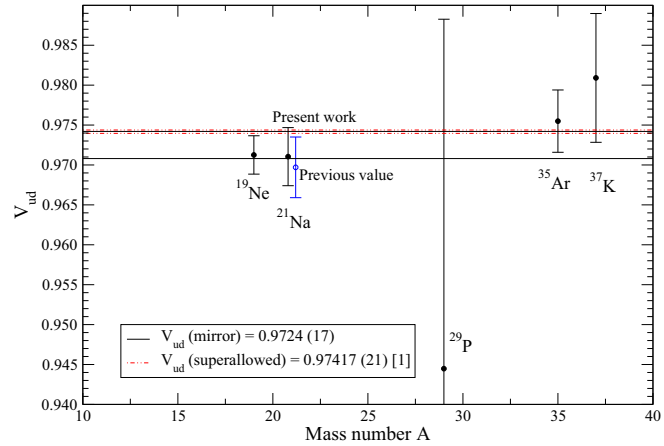

FIG. 8. (Color online) V_{ud} values for $T = 1/2$ mirror nuclei (solid and dashed lines shown here are the total uncertainty ranges of the corresponding averaged V_{ud} values). The deduced values for ^{19}Ne and ^{37}K are updated with the most recent measurements [6–9]. The previous value of V_{ud} for ^{21}Na is deduced using Refs. [4,5]. The present V_{ud} value of ^{21}Na is in excellent agreement with that of the most precisely known value of ^{19}Ne, and shifts the value of V_{ud} from mirror transitions into better agreement with the value obtained from superallowed 0^+ to 0^+ transitions.

This new value (compared to the previous value of 6202 (48) s for ^{21}Na [4]) is in excellent agreement with the $\mathcal{F}t_0$ value of 6182 (28) s for ^{19}Ne (calculated in the present work using the most recent experimental measurements [6–8]). Combining the $\mathcal{F}t_0$ values for ^{19}Ne, ^{21}Na (present work), ^{29}P, ^{35}Ar, and ^{37}K, the weighted average $\mathcal{F}t_0$ value for all $T = 1/2$ mirror transitions is 6167 (21) s.

The value of V_{ud} from ^{21}Na alone can now be deduced by combining Eqs. (1) and (5). The result of

$$V_{\text{ud}} = 0.9710(36), \quad (7)$$

can be compared to the previous value of 0.9697 (38) for ^{21}Na determined using the previous average half-life from Ref. [5]. The uncertainty on this new value is not significantly improved, because the uncertainty in V_{ud} is dominated by the experimentally determined correlation parameters from which the value of ρ is deduced.

Figure 8 shows the values for all $T = 1/2$ mirror nuclei presently considered in the evaluation of V_{ud} [4], all of which have been updated using the most recent measurements [6–9]. The value of V_{ud} from the present work is in excellent agreement with that of the most precisely known value from ^{19}Ne and is now better aligned with the other mirror nuclei. The weighted average of all V_{ud} values, determined to be 0.9724 (17), is now in better agreement with the V_{ud} of 0.97417 (21) [1] from superallowed 0^+ to 0^+ nuclear β decays.

Conclusion. A high-precision half-life measurement was performed for the $T = 1/2$ mirror nucleus ^{21}Na with the aim of improving the precision of the $\mathcal{F}t^{\text{mirror}}$ value, which is in turn used to derive V_{ud}. The new half-life was determined to be $T_{1/2} = 22.422$ (10) s, which represents a result that is precise to 0.04% and is an improvement by more than a factor of 5

over the previous world average [5], allowing the precision of the $\mathcal{F}t^{\text{mirror}}$ for the ^{21}Na decay to be reduced to 0.15%, to what is now the second most precise $\mathcal{F}t^{\text{mirror}}$ value. As a result, the value of $\mathcal{F}t_0$ and V_{ud} for ^{21}Na decay are now in better agreement with the values derived from ^{19}Ne; however, the uncertainty is still dominated by the precision of the correlation parameters. New measurements of these parameters will be possible at the GANIL-SPIRAL facility using the LPCTrap device [21] and will improve the precision with which V_{ud} can be determined for ^{21}Na.

Acknowledgments. We thank the GANIL accelerator and technical staff for their hard work and support. We are especially grateful to B. Blank and E. Liénard for helpful discussions.

[1] J. C. Hardy and I. S. Towner, Phys. Rev. C **91**, 025501 (2015).
[2] F. E. Wietfeldt and G. L. Greene, Rev. Mod. Phys. **83**, 1173 (2011).
[3] A. R. Young *et al.*, J. Phys. G: Nucl. Part. Phys. **41**, 114007 (2014).
[4] O. Naviliat-Cuncic and N. Severijns, Phys. Rev. Lett. **102**, 142302 (2009).
[5] N. Severijns, M. Tandecki, T. Phalet, and I. S. Towner, Phys. Rev. C **78**, 055501 (2008).
[6] P. Ujić *et al.*, Phys. Rev. Lett. **110**, 032501 (2013).
[7] S. Triambak *et al.*, Phys. Rev. Lett. **109**, 042301 (2012).
[8] L. J. Broussard *et al.*, Phys. Rev. Lett. **112**, 212301 (2014).
[9] P. D. Shidling *et al.*, Phys. Rev. C **90**, 032501(R) (2014).
[10] N. L. Achouri *et al.*, J. Phys. G: Nucl. Part. Phys. **37**, 045103 (2010).
[11] P. A. Vetter, J. R. Abo-Shaeer, S. J. Freedman, and R. Maruyama, Phys. Rev. C **77**, 035502 (2008).
[12] V. E. Iacob *et al.*, Phys. Rev. C **74**, 015501 (2006).
[13] S. E. Arnell, J. Dubois, and O. Almén, Nucl. Phys. **6**, 196 (1958).
[14] D. E. Alburger, Phys. Rev. C **9**, 991 (1974).
[15] G. Azuelos and J. E. Kitching, Phys. Rev. C **12**, 563 (1975).
[16] L. Penescu, R. Catherall, J. Lettry, and T. Stora, Rev. Sci. Instrum. **81**, 02A906 (2010).
[17] G. F. Grinyer *et al.*, Nucl. Instrum. Methods Phys. Res., Sect. A **741**, 18 (2014).
[18] G. F. Grinyer *et al.*, Phys. Rev. C **71**, 044309 (2005).
[19] V. T. Koslowsky *et al.*, Nucl. Instrum. Methods A **401**, 289 (1997).
[20] K. A. Olive *et al.*, Chin. Phys. C **38**, 090001 (2014).
[21] G. Ban *et al.*, Ann. Phys. (Berlin) **525**, 576 (2013).